Civil and Environmental Engineering
Vol. 21, Issue 1, 680-688, DOI: 10.2478/cee-2025-0061

VERIFICATION OF THE APPLICATION OF MACDRAIN® W1071 I DRAINAGE GEOCOMPOSITE IN SUB-BALLAST LAYERS

Libor IŽVOLT[1], Peter DOBEŠ[1,*], Martin MEČÁR[1], Joanna GRZYBOWSKA-PIETRAS[2]

[1] Faculty of Civil Engineering, University of Žilina, Univerzitná 8215/1, 010 26 Žilina, Slovakia.
[2] Faculty of Materials, Civil and Environmental Engineering, University of Bielsko-Biala, Willowa 2, 43-309 Bielsko-Biala, Poland.
[*] corresponding author: peter.dobes@uniza.sk

Abstract

The research of the Department of Railway Engineering and Track Management (DRETM) has long been focused on evaluating the potential application of various thermal insulating, reinforcing, or composite building materials in the construction of the sub-ballast layers. For this purpose, an experimental facility called the DRETM Test Stand was built on the campus of the University of Žilina (UNIZA), consisting of eight measurement profiles (test fields). Each measurement profile is characterized by its specific construction and material composition. The application of construction materials that have not yet been applied within the Slovak Railways network, such as extruded polystyrene, Liapor, Liapor concrete, foam concrete, and foam glass, is mainly evaluated within the individual measurement profiles.
At the request of MACCAFERRI CENTRAL EUROPE, s.r.o., the drainage geocomposite MacDrain® W1071 was tested on the aforementioned test stand to assess its potential application in the sub-ballast layers. This drainage geocomposite is primarily designed to ensure drainage and separation functions within the construction of the sub-ballast layers. The article evaluates its potential use as a thermal layer to potentially increase the thermal resistance of the trackbed construction. In other words, it considers whether its application could enhance the protection of the subgrade surface of fine-grained soils not only against the adverse effects of water but also against frost.

Keywords:

Sub-ballast layers; Measurement profile, Drainage geocomposite; Thermal-technical properties; Frost depth.

1 Introduction

A common cause of geometric track position defects is the presence of fine-grained materials in the subgrade (particularly on the subgrade surface) of railway tracks and their insufficient protection not only against water but also against frost. The thermal resistance of trackbed, or the sub-ballast layers, primarily depends on the thickness and thermal conductivity coefficient of individual structural layers. When thermal insulation materials with a thermal conductivity coefficient $\lambda < 0.4$ $W \cdot m^{-1} \cdot K^{-1}$ (e.g., expanded or extruded polystyrene, polyurethane, Liapor, foam glass, composite foam concrete, etc.) are applied in the sub-ballast layers, it is possible to reduce their structural thickness compared to a situation where the sub-ballast layers of the railway comprise solely standard natural materials (crushed stone/aggregate or gravel-sand mixtures).

The construction market currently offers various types of thermal insulation materials with different material compositions and technical properties. Since most developed countries worldwide strive to ensure sustainable development and conserve natural resources, recycled sources (e.g., foam glass production) or foaming agents (e.g., composite foam concrete production) are often used in the manufacturing of construction materials, including thermal insulation materials. At the Department of Railway Engineering and Track Management (DRETM), research has long focused on the possibilities of applying various construction materials (thermal insulation, reinforcement, or materials from recycled components) in the railway substructure, or the protective formation layer. For this purpose, an experimental facility called DRETM Test Stand (Figures 1 and 6, bottom left) was established. It consists of three different sectors (sectors A, B, and C), which allow for experimental monitoring and assessment of the deformation and thermal insulation properties of various construction materials. Section A is designed for monitoring the thermal insulation properties of built-in thermal insulation materials in a full-scale railway track construction model (1:1 scale). It contains a total of eight measurement profiles (MPs), each characterized by a specific structural and material composition. These measurement profiles typically assess the application of construction materials that have not yet been implemented within the Slovak Railways network, such as extruded polystyrene, Liapor, Liapor concrete, foam concrete, and foam glass. Detailed information on the structural and material composition of the individual measurement profiles, including experimental measurement results and numerical modeling, is provided and analyzed in detail in reference [1].

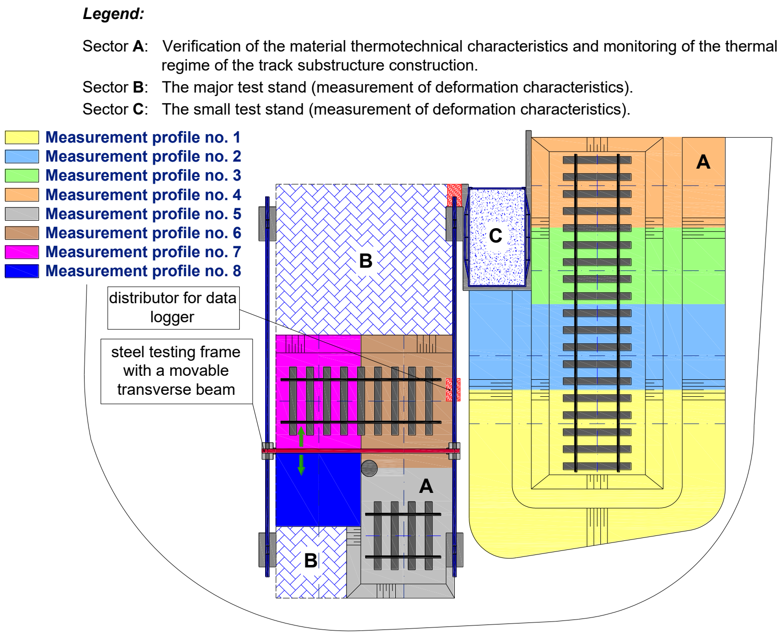

Fig. 1: DRETM Test Stand.

This article focuses on the most recently built measurement profile no. 8 (MP 8), which is characterized by the incorporation of the MacDrain® W 1071 I drainage geocomposite into the sub-ballast layers (marked in dark blue in sector A). This drainage geocomposite is designed to provide drainage and separation functions within the structural composition of the sub-ballast layers. MACCAFERRI CENTRAL EUROPE, s.r.o., requested further assessment to determine whether this geocomposite could also influence the thermal resistance of the track substructure. Unlike MP 1 to MP 7, the railway superstructure in MP 8 does not include a track skeleton, only a ballast layer. This design allows for the potential replacement of the assessed material with a different type of geosynthetic material based on experimental findings. Additionally, in general, this composition enables testing of other thermal insulation construction materials. However, it should be emphasized that in this case, the structural composition does not significantly influence the observed characteristics or properties of the tested material.

The application of geocomposite materials in transport infrastructure is being researched in several countries, including Slovakia. For example, in Portugal, research has focused on assessing the resistance of geocomposites to mechanical damage (repeated loading or abrasion resistance). Changes in geocomposites during tensile and tearing tests were observed. The results indicated that degradation tests often caused a deterioration of geocomposite properties under tension and tearing, affecting its reinforcement function [2]. In the USA, research has primarily examined the drainage properties of embedded geocomposites in road construction. Studies have shown that geocomposites increased the permeability of road structures by two to three times, effectively preventing the saturation of surface materials and subgrade during heavy rainfall [3]. In Italy, research has also focused on the application of drainage geocomposites in road construction to prevent pavement deformations caused by frost. Findings revealed that frost does not affect drainage efficiency, while embedded geocomposites reduced frost heave height and interrupted capillary rise [4, 5].

Additionally, in Italy, four different geocomposites combining reinforcement geosynthetics with a bitumen membrane were examined for their effect on crack propagation and the bonding of asphalt pavement layers. Research results demonstrated that embedded geocomposites significantly extended pavement lifespan. However, they also weakened the interlayer bonding of asphalt layers, reducing pavement stiffness [6].

In Iraq, research assessed the performance of soil reinforcement using three different types of geosynthetics, including a geocomposite. The study concluded that both reinforcement geocomposites and geogrids positively impacted the deformation resistance of the structure [7].

Similarly, in Slovakia, research has been conducted on embedding various geosynthetic materials into five different soil types (ash, sand, and gravels of various grain sizes) and assessing their shear strength. Results indicate that the correct placement of geosynthetics and proper compaction techniques (especially for well-graded coarse-grained materials) significantly influence shear strength. In general, the interface coefficient (α) of geosynthetics with their surroundings increases as particle size decreases and with poor gradation [8].

In the UK, research has focused on the application of polyurethane geocomposites in the structural composition of high-speed railway tracks with ballast beds to maintain track geometry quality. The findings suggest that this material has significant potential for stabilizing track geometry under high-speed conditions [9].

In Portugal, researchers have developed a self-sensing cementitious geocomposite consisting of stabilized cemented sand with multi-walled carbon nanotubes (MWCNTs) and graphene nanoplatelets (GNPs) as conductive fillers. This geocomposite could be used for detecting structural layer damage in railway tracks [10].

In the Czech Republic, studies examined the application of stabilized hexagonal geocomposites in railway track structures to improve stability and prevent fine soil particle migration from the subgrade into the ballast. Research results indicate that this solution is effective in problematic areas of railway tracks regarding stability [11].

2 Test material and method

The test samples of the MacDrain® W 1071 I drainage geocomposite (Fig. 2) used in our research were obtained from MACCAFERRI CENTRAL EUROPE, s.r.o. The MacDrain® W 1071 I drainage geocomposite (GCD) is manufactured through a continuous thermal bonding process, integrating a drainage core (extruded polymer monofilaments – GMA, shaped into a "W" profile with parallel channels), which is positioned between two layers of geotextile (GTX) [12]. The fundamental physical properties of the drainage geocomposite are presented in Table 1.

Fig. 2: Test sample (drainage geocomposite MacDrain® W 1071 I).

Table 1: Basic physical properties of the drainage geocomposite MacDrain® W 1071 I [12].

Thickness under 2 kPa load	[mm]	EN ISO 9863-1	6.9 (±10%)
Thickness under 20 kPa load	[mm]	EN ISO 9863-1	-
Areal mass / Surface density	[$g \cdot m^{-2}$]	EN ISO 9864	720 (± 10%)
Tensile strength	[$kN \cdot m^{-1}$]	EN ISO 10319	20.0 (-6.0)
In-plane drainage capacity	[$l \cdot m^{-1} \cdot s^{-1}$]	EN ISO 12958	0.18 – 2.44 (±25%)*
Flow reduction factor due to creep under 100 kPa load for a design life of 100 years	[-]	ISO 25619-1	< 1.15

* Value dependent on slope, type of contact (soft/soft, rigid/soft), and installation time

At a partner research facility in Poland, specifically at the University of Bielsko-Biała, the first step of the joint research project involved determining the thermal conductivity coefficient (λ) and thermal resistance (R) of the tested MacDrain® W 1071 I drainage geocomposite in its dry state. This was carried out using a Heat Flow Meter LM.PLUS 305 (Fig. 3).

Fig. 3: Heat Flow Meter LM.PLUS 305.

The device compresses the test sample between two pressing plates (upper and lower plates of the device) and allows for the measurement of test samples with a maximum thickness of 100 mm and a minimum width/length of 300 mm. The temperature of the upper plate can be set between 5 and 50 °C (with a default setting of 15 °C), while the temperature of the lower plate can be adjusted from -5 to 40 °C (default setting: 5 °C). The device maintains a constant temperature on both sides of the tested sample, with fluctuations of less than ±0.01 °C from the set value. The measurement range of the device is from 1/3 to 800 $W \cdot m^{-1} \cdot K^{-1}$. Heat flux is measured using two separate heat flux sensors [13].

Since this device does not allow for measurements on samples in a wet state (due to possible condensation on the pressing plates and subsequent damage to the device's sensors), which is the typical condition when embedded in a sub-ballast layers, the drainage geocomposite was incorporated into a full-scale 1:1 railway track construction model — measurement profile no. 8 (MP8, Fig. 4) — at the DRETM experimental facility.

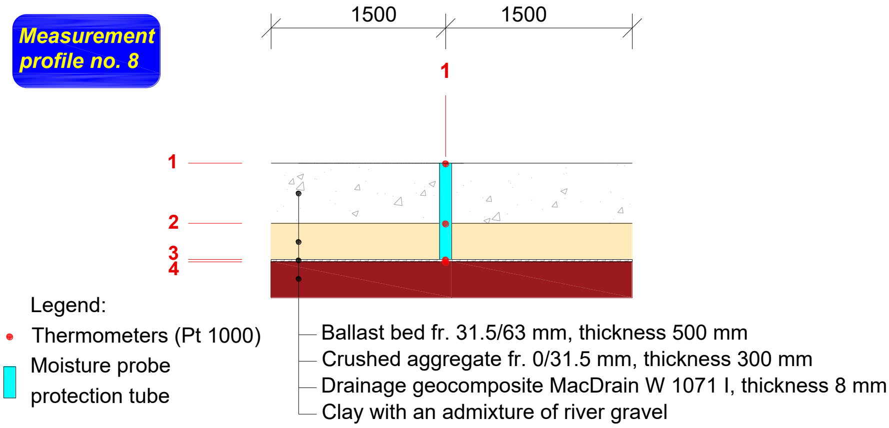

Fig. 4: Measurement profile no. 8 with built-in drainage geocomposite – structural composition.

Structurally, MP8 represents a railway track constructed in a cut. The material composition of MP8 consists of a ballast bed with a fraction of 31.5/63 mm and a thickness of 500 mm, a protective layer of crushed aggregate with a fraction of 0/31.5 mm and a thickness of 300 mm, the drainage geocomposite MacDrain® W 1071 I, and a subgrade composed of clay with an admixture of river gravel (frost-susceptible subgrade surface).

The MP8 structure includes four Pt1000 resistance ground temperature sensors installed at different locations: on the ballast surface, at the level of the sub-ballast upper surface, on the surface of the geocomposite, and on the underside of the geocomposite (i.e., on the subgrade surface level). The

Pt1000 temperature sensors (Fig. 5, left) enable temperature measurements in the range of -55 to 125 °C, with an accuracy of ±0.5 °C within the range of -10 to 85 °C. These sensors are connected to a data logger (dataTaker DT80) via a CEM20 channel expansion module (Fig. 5, center). In our case, temperature data are recorded every 30 minutes (although the logging interval can be adjusted to a shorter or longer duration), which is a sufficiently relevant time interval for measurement purposes.

The dataTaker DT80 logger operates in environments with temperatures ranging from -45 to 70 °C and a relative humidity of up to 85% (provided that condensation does not occur in this environment) [14]. Additionally, air temperature and relative humidity measurements are conducted (to evaluate the climatic characteristics of winter periods) using a Comet T3419 sensor housed in a specialized meteorological shield, positioned 2.0 m above ground level (Fig. 5, right). This sensor can record temperatures ranging from -30 to 105 °C, with an accuracy of ±0.4 °C [15]. Figure 6 presents images from the construction of MP8.

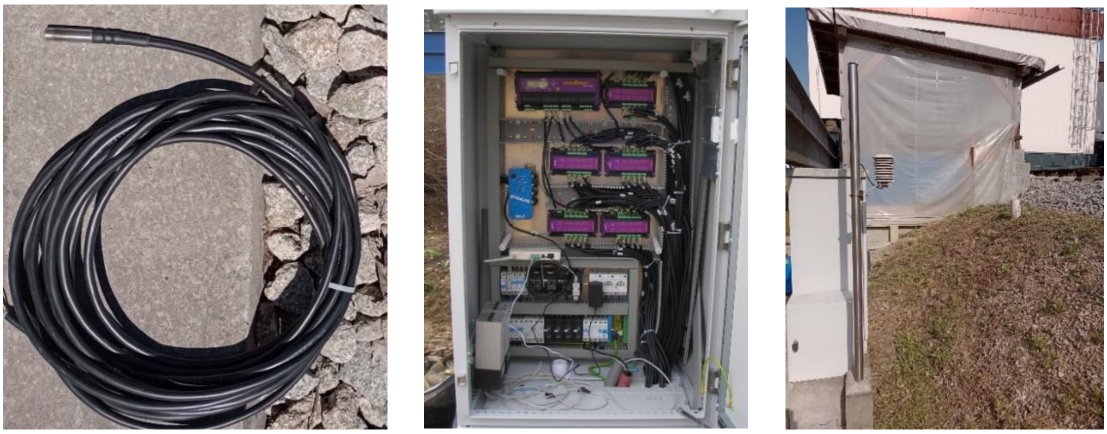

Fig. 5: Measuring equipment - Pt 1000 resistance ground temperature sensor (left), connection of the temperature sensors to the dataTaker DT80 logger via the CEM20 channel expansion modules (center), Comet T3419 sensor housed in a specialized meteorological shield (right).

Fig. 6: Construction of MP8 – application of drainage geocomposite on the subgrade surface level with installation of temperature sensors (top left), installation of temperature sensor at the level of the sub-ballast upper surface (top right), overall view of the DRETM Test Stand (bottom left), detailed view of MP8 (bottom right).

3 Results and Discussion

Some physical and thermal-technical parameters of the drainage geocomposite MacDrain® W 1071 I in a dry state were initially tested using a heat flow measurement device (see Fig. 3). Details of the device and measurement method are provided in Section 2. Table 2 presents the measurement results.

Table 2: Determined physical and thermal-technical parameters of the drainage geocomposite MacDrain® W 1071 I.

Sample number	**Dimensions**	**Thickness**	**Mass *m***	**Bulk density ρ**	**Thermal conductivity coefficient λ**	**Thermal resistance *R***	**Heat flux density *q***
	[mm]	[mm]	[g]	[kg·m^{-3}]	[W·m^{-1}·K^{-1}]	[m^{2}·K·W^{-1}]	[W·m^{-2}]
1	390x400	7.9	117.9	95.4	0.0458	0.17	50.52
2	400x410	8.1	113.7	85.9	0.0459	0.18	49.87

The values presented in Table 2 indicate that the drainage geocomposite MacDrain® W 1071 I exhibits excellent thermal insulation properties in a dry state. However, since this geosynthetic material is primarily used to ensure a drainage function—i.e., to accumulate and channel water—it is logical that within the structure of a railway track, which inherently represents an open system (where all water, whether from rain or snow, infiltrates the traditional railway track structure), it will never remain in a completely dry state.

For this reason, it was necessary to assess its thermal insulation properties in a wet state. However, the heat flow measurement device does not allow for such testing.

To evaluate the effect of the drainage geocomposite MacDrain® W 1071 I on the thermal resistance of the sub-ballast layers in its wet state, the previously mentioned MP8 was constructed. The structural and material composition of MP8, as well as the measurement techniques used, are further specified in Section 2.

The thermal-technical properties of the drainage geocomposite are best assessed during an actual winter period, particularly one in which the highest possible air frost index I_F is reached or in which a prolonged (main) frost period can be identified. Since MP8 was constructed in 2023, at the time of writing this paper, only one winter period—2023/2024—had been recorded and analyzed for MP8. Table 3 presents the determined climatic characteristics of the winter period 2023/2024.

Table 3: Determined climatic characteristics of the winter period 2023/2024 for the MP8.

Winter period	**Minimum average daily air temperature θ_s**	**Average annual air temperature θ_m**	**Air frost index I_F**	**Surface air frost index $I_{F,S}$**	**Frost penetration depth D_F**
	[°C]	[°C]	[°C, day]	[°C, day]	[m]
2023/2024	-8.30	10.15	49	63	0.53

Figure 7 presents an evaluation of the main monitored climatic parameters of the winter period 2023/2024, specifically the air frost index (Figure 7, left) and the frost penetration depth of the structure (Figure 7, right).

From Figure 7 (left), it is evident that the achieved air frost index I_F during the winter of 2023/2024 was very low, reaching only about 10% of the design value for the Žilina region ($I_{F,D}$ = 480 °C, day), where MP8 is located. Consequently, the 0 °C isotherm penetrated only slightly below the formation level, resulting in frost penetration limited to the ballast layer (Figure 7, right).

The observed climatic characteristics are insufficient for a comprehensive or definitive assessment of MP8 in terms of resistance to climatic loads. However, by comparing the determined climatic characteristics and the measured temperatures in the individual structural layers with those recorded for MP5 (a standard sub-ballast layers where the protective layer consists solely of crushed aggregate, fraction 0/31.5 mm), as well as with over 20 years of experimental measurements monitoring the effects of frost on frost penetration depth and the thermal resistance of railway track structures, certain conclusions can still be drawn.

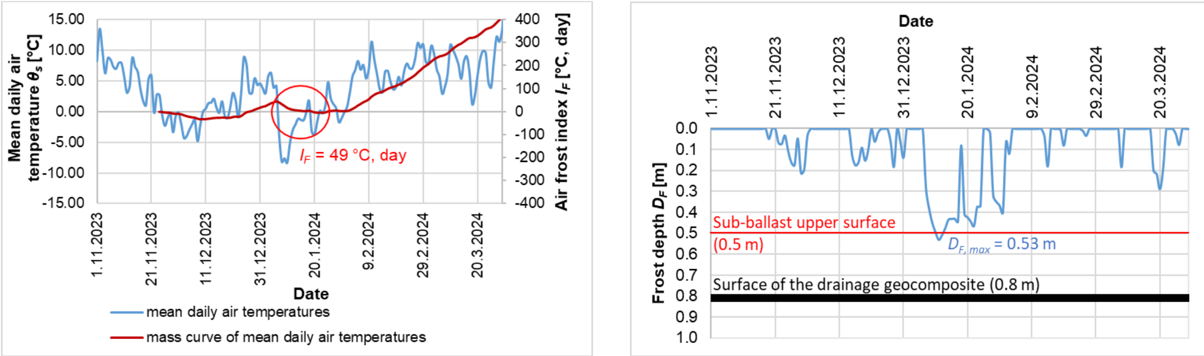

Fig. 7: Evaluation of the air frost index I_F (left), evaluation of the structure frost depth D_F (right).

In MP5, the achieved frost penetration depth D_F was 0.43 m, which is 0.10 m less than that observed in the MP8 structure. Based on long-term experience with various thermal insulation materials embedded in railway substructure construction—such as extruded polystyrene, foam glass, expanded clay (Liapor), and composite foam concrete—previously published multiple times by the authors, it is evident that thermal insulation materials prevent cold penetration into the subgrade. However, this results in increased frost penetration in the overlying layers.

Therefore, if the railway track structure is not exposed to climatic conditions severe enough to cause frost penetration below the thermal insulation material, the frost penetration depth in such a structure will always be greater than in a standard sub-ballast layers without embedded thermal insulation material.

The key parameter for confirming the thermal insulation effect of a material within the railway substructure—specifically its ability to protect the frost-susceptible subgrade surface from freezing—is the temperature measured beneath the thermal insulation material. In a modified structure where thermal insulation material is applied, the temperature beneath it must be higher than at the same depth in a standard structure without insulation material. For instance, in cases where extruded polystyrene was embedded, the temperature remained 1 to 4 °C higher throughout the year. Figure 8 presents a comparison of the relevant temperatures recorded in MP5 and MP8.

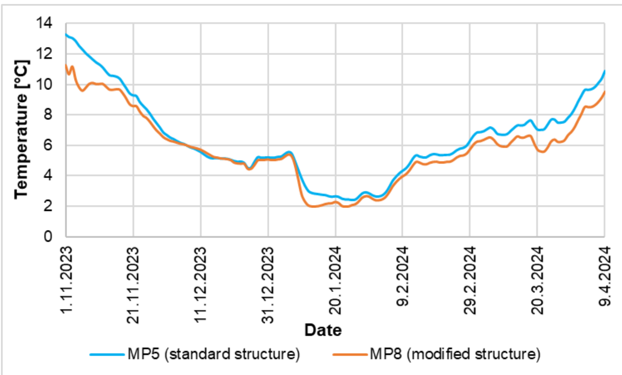

Fig. 8: Comparison of measured temperatures under the drainage geocomposite (MP8) and at the same depth level in MP5 during the winter period 2023/2024.

The main frost period of the winter season 2023/2024, during which the maximum air frost index I_F and the frost penetration depth D_F were recorded, lasted from January 7, 2024, to January 24, 2024.

As shown in Figure 8, during this main frost period, the temperature measured beneath the drainage geocomposite was 0.2 to 1.0 °C lower— which is an opposite effect compared to other embedded thermal insulation materials. Based on these temperature measurements, it can be assumed that the greater frost penetration depth D_F observed in MP8 was caused by its lower thermal insulation properties in a wet state. This is logical, as water has poorer thermal insulation properties than air.

4 Conclusions from the analysis

The aim of this publication was to assess the potential impact of the drainage geocomposite MacDrain® W 1071 I on the thermal resistance of the track substructure, specifically the trackbed, which is typically influenced by the incorporation of various thermal insulation materials or structural layers. In addition to protecting the frost-susceptible subgrade surface, an ideal solution would also achieve a reduction in its overall thickness (which is traditionally constructed using natural materials such as crushed aggregate or gravel-sand mixtures), thereby conserving natural material resources.

Experimental measurements using a heat flow meter (Figure 3) demonstrated that the tested drainage geocomposite MacDrain® W 1071 I exhibits excellent thermal insulation properties in a dry state (see Table 1). However, it was not possible to conduct measurements on wet samples using the Heat Flow Meter LM.PLUS 305. Therefore, the drainage geocomposite was embedded in a full-scale track substructure model (DRETM Test Stand, MP8) to assess its performance under real climatic conditions, albeit only for a single winter period.

Although the climatic load during the monitored winter period of 2023/2024 was relatively low, based on the measured values and long-term experience from the DRETM Test Stand, as well as numerical modeling of the thermal behavior of railway structures with embedded thermal insulation materials, it can be assumed that the tested drainage geocomposite MacDrain® W 1071 I alone is unlikely to have a direct impact on improving the protection of the frost-susceptible subgrade surface against the effects of frost.

However, ultimately, it can be assumed that the incorporation of the drainage geocomposite will have a generally positive impact on the trackbed construction in several aspects. This is due to the fact that, thanks to the excellent drainage function of the geocomposite (placed above the subgrade surface), confirmed by the research results presented in Chapter 1 (literature [3], [4], [5]), the materials in the trackbed layers will remain in a relatively dry state for an extended period. As a result, they will not accumulate excess water but will maintain their natural moisture content.

This influences their lower thermal conductivity, thereby increasing the required thermal resistance of the trackbed construction.

An additional significant benefit of the MacDrain® W 1071 I geocomposite is that its drainage effect prevents excessive water saturation of the subgrade surface, allowing it to maintain only its natural moisture content. This stabilizes its deformation resistance over time, ensuring the necessary stability of the railway track. Ultimately, this will impact the operational safety and reliability of the track. The conservation of natural construction material resources used in railway track construction can also be achieved by reducing the proposed thickness of the sub-ballast layer, as its thickness depends on the overall resistance of the designed structure to operational (static and dynamic) loading. In the case of the MacDrain® W 1071 I geocomposite, the savings in construction materials were assessed with respect to the reduction of the proposed structural thickness of the sub-ballast (protective) layer depending on the applied non-traffic load (thermal-technical parameters of the materials).

Therefore, as part of future research at our institution, the latest type of drainage geocomposite will be tested, specifically the reinforcement-drainage multi-composite MacDrain™ W09.EG2S (Figure 9), which contains, in addition to the drainage core and two filtering nonwoven geotextiles, a reinforcing stabilizing polypropylene biaxial extruded geogrid. This material could have a favorable effect on achieving the desired deformation parameters of the subgrade, improving stress distribution, and limiting uneven settlement of railway track construction on poorly deformable subgrade surfaces, which are characteristic of fine-grained frost-susceptible soils.

Fig. 9: Drainage multicomposite MacDrain™ I W09.EG2S.

References

[1] IŽVOLT, L. – DOBEŠ, P. – MEČÁR, M. – NAVIKAS, D.: Analysis of the Influence of Incorporating Different Thermal-Insulating Materials into the Sub-Ballast Layers. Buildings, Vol. 15, Iss. 2, 2025, pp. 1-26, https://doi.org/10.3390/buildings15020239.

[2] CARNEIRO, J.R. – ALMEIDA, F. – CARVALHO, F. – LOPES, M.L.: Tensile and Tearing Properties of a Geocomposite Mechanically Damaged by Repeated Loading and Abrasion. Materials, Vol. 16, Iss. 21, 2023, pp. 1-19, https://doi.org/10.3390/ma16217047.

[3] LI, CH. – ASHLOCK, J. – WHITE, D. – VENNAPUSA, P.: Permeability and Stiffness Assessment of Paved and Unpaved Roads with Geocomposite Drainage Layers. Applied Sciences, Vol. 7, Iss. 7, 2017, pp. 1-15, https://doi.org/10.3390/app7070718.

[4] FERRARA, M. – TROVATO, F.: The Use of Drainage Geocomposites in Cold Regions. E3S Web of Conferences, Vol. 569, 2024, pp. 1-10, https://doi.org/10.1051/e3sconf/202456902004.

[5] RIMOLDI, P. – PEZZANO, P. – MARTINO, I. – SCOTTO, M.: Development and Application of an Engineered Drainage Geocomposite for the Control of the Frost Heave in Road Structures in Arctic Regions. Proceedings of the 4th Pan American Conference on Geosynthetics, Rio de Janeiro, Brazil, 26-29 April 2020, pp. 1-10.

[6] SPADONI, S. – INGRASSIA, L.P. – PAOLINI, G. – VIRGILI, A. – CANESTRARI, F.: Influence of Geocomposite Properties on the Crack Propagation and Interlayer Bonding of Asphalt Pavements. Materials, Vol. 14, Iss. 18, 2021, pp. 1-18, https://doi.org/10.3390/ma14185310.

[7] ABDI-GOUDARZI, S. – ZIAIE-MOAYED, R. – NAZERI A.: An Experimental Evaluation of Geocomposite-Reinforced Soil Sections. Construction and Building Materials, Vol. 314, 2022, pp. 1-12, https://doi.org/10.1016/j.conbuildmat.2021.125566.

[8] STACHO, J. – SULOVSKA, M. – SLAVIK, I.: Analysis of the Shear Strength of a Soil-Geosynthetic Interface. Civil and Environmental Engineering, Vol 19, Iss. 1, 2023, pp. 452-463, https://doi.org/10.2478/cee-2023-0040.

[9] WOODWARD, P.K. – KACIMI, A. – LAGHROUCHE, O. – MEDERO, G.M. – BANIMAHD, M.: Application of Polyurethane Geocomposites to Help Maintain Track Geometry for High-Speed Ballasted Railway Tracks. Journal of Zhejiang University – Science A: Applied Physics & Engineering, Vol. 13, Iss. 11, 2012, pp. 836-849, https://doi.org/10.1631/jzus.A12ISGT3.

[10] CORREIA, A.G. – ROSHAN, M.J.: Self-Sensing Cementitious Geocomposites in Rail Track Substructures. Transportation Geotechnics, Vol. 46, 2024, pp. 1-23, https://doi.org/10.1016/j.trgeo.2024.101260.

[11] HORNÍČEK, L. – BŘEŠŤOVSKÝ, P. – JASANSKÝ, P.: Application of Geocomposite Placed beneath Ballast Bed to Improve Ballast Quality and Track Stability. IOP Conference Series: Materials Science and Engineering, Vol. 236, 2017, pp. 1-8, https://doi.org/10.1088/1757-899X/236/1/012039.

[12] MACCAFERRI: Product Data Sheet for MacDrain W 1071 I.

[13] STIROLAB: Heat Flow Meters, https://www.stirolab.com/heat-flow-meters.html.

[14] CAS DATALOGGERS: DataTaker CEM20, https://dataloggerinc.com/product/cem20-20-channel-expansion-module/?srsltid=AfmBOorcK7B10ALIVWP3TOGypsy4MtfAi_j8ZSAwDaNe65R-9RN6UiaO.

[15] COMET: Temperature and Humidity Sensor with RS485 Output, https://www.cometsystem.cz/reg-T3419?gad_source=1&gclid=EAIaIQobChMIv8zj3L_4igMVzqeDBx1QaDGFEAAYASAAEgJh2_D_BwE.